ARTICLES
PUBLISHED ONLINE: 3 FEBRUARY 2015 | DOI: 10.1038/NGEO2343
nature geoscience

Randomness of megathrust earthquakes implied by rapid stress recovery after the Japan earthquake

Thessa Tormann[1]*, Bogdan Enescu[2], Jochen Woessner[3] and Stefan Wiemer[4]

Constraints on the recurrence times of subduction zone earthquakes are important for seismic hazard assessment and mitigation. Models of such megathrust earthquakes often assume that subduction zones are segmented and earthquakes occur quasi-periodically owing to constant tectonic loading. Here we analyse the occurrence of small earthquakes compared to larger ones—the *b*-values—on a 1,000-km-long section of the subducting Pacific Plate beneath central and northern Japan since 1998. We find that the *b*-values vary spatially and mirror the tectonic regime. For example, high *b*-values, indicative of low stress, occur in locations characterized by deep magma chambers and low *b*-values, or high stress, occur where the subducting and overriding plates are strongly coupled. There is no significant variation in the low *b*-values to suggest the plate interface is segmented in a way that might limit potential ruptures. Parts of the plate interface that ruptured during the 2011 Tohoku-oki earthquake were highly stressed in the years leading up to the earthquake. Although the stress was largely released during the 2011 rupture, we find that the stress levels quickly recovered to pre-quake levels within just a few years. We conclude that large earthquakes may not have a characteristic location, size or recurrence interval, and might therefore occur more randomly distributed in time.

Elastic rebound theory, introduced first by Reid following the 1906 San Francisco earthquake[1], is one of the foundations of earthquake science and explains how tectonic forces load faults. It states that tectonic stresses build up on a fault over decades, to be released within a major earthquake in seconds. However, it is still unknown if this release is complete and followed by a period of gradual reloading—and thus relative safety—or if sufficient energy remains in the system to allow similar size events more or less immediately. To explore this question, we use a fundamental observation in seismology, the exponential relationship between the frequency and magnitude of earthquakes, known as Gutenberg–Richter law[2], $\log_{10}(N) = a - bM$, where N is the number of events equal or above magnitude M, and a and b are constants. This relationship is commonly used to infer occurrence rates of infrequent large and hazardous events from the productivity level (a-value) and size distribution (b-value) of abundant small-to-moderate-magnitude seismicity. Although on a global average $b \approx 1$, local b-values show substantial spatial variations—that is, in some volumes the proportion of larger magnitudes is higher ($b < 1$), in others the proportion of small magnitudes exceeds the average expectation ($b > 1$).

Evidence from laboratory experiments[3,4], numerical modelling[5], and natural seismicity[6–8] indicates that b-values are negatively correlated with differential stress. Fault patches of such-determined significant stress accumulation have been observed to coincide with locations of subsequent large earthquakes[9,10]. Low differential stress conditions, for example, in high-pore-pressure regimes, lead to high b-values, as observed in geothermal[11] and volcanic[6] settings. These observations suggest the use of b-values for mapping the heterogeneous stress conditions in the Earth's crust.

Spatial variation: time-invariant tectonic footprint

Our b-value study along the subducting Pacific plate off Japan is the first of its kind to demonstrate how large-scale seismotectonics imprint on the relative size distribution of earthquakes (for details on the applied mapping, see Methods). We find the following three major structural expressions, resolved with spatially varying coverage, for any time period that we chose (Figs 1 and 2).

First, we observe a relatively homogeneous band of high b-values at depths below ~100 km following the volcanic front (Figs 1 and 2, $b > 1.1$). This structure represents the origin of the deep magmatic root feeding the magma chambers of the volcanic chain[6,12,13]: dehydration and partial melting of the subducting slab releases material that ascends and eventually feeds the volcanoes above. Increasing pore pressures reduce differential stresses and b-values increase, as observed also during geothermal injection experiments[11]. The b-values for crustal earthquakes below the volcanoes are equally high, as shown along a cross-section at 40° N (inset Fig. 1, $b > 1.1$). Latest volcanic activity/unrest along this cross-section has been reported in the late 1990s (www.volcanodiscovery.com).

Second, we image large volumes of low and very low b-values from ~100 km depth up to the trench (Figs 1 and 2, $b < 0.9$). The shallower part of the subduction interface is where the plates are strongly coupled, although with significant depth and lateral variations, and the accumulating stresses are released infrequently by large or megathrust earthquakes[14]. Within this low-b-value regime, we do not observe any significant segmentation that would suggest inherent limits to potential ruptures. From the short available observation period for estimating the depth extent of co-seismic rupture from large subduction zone earthquakes, at depths down to about 60 km (ref. 15). We image low b-values down

[1]ETH Zurich, Swiss Seismological Service, Sonneggstrasse 5, Zürich 8092, Switzerland. [2]University of Tsukuba, Faculty of Life and Environmental Sciences, 1-1-1 Tennodai, Tsukuba, Ibaraki 305-8572, Japan. [3]Risk Management Solutions Inc., Stampfenbachstrasse 85, Zürich 8006, Switzerland. [4]ETH Zurich, Swiss Seismological Service, Sonneggstrasse 5, Zürich 8092, Switzerland. *e-mail: thessa.tormann@sed.ethz.ch

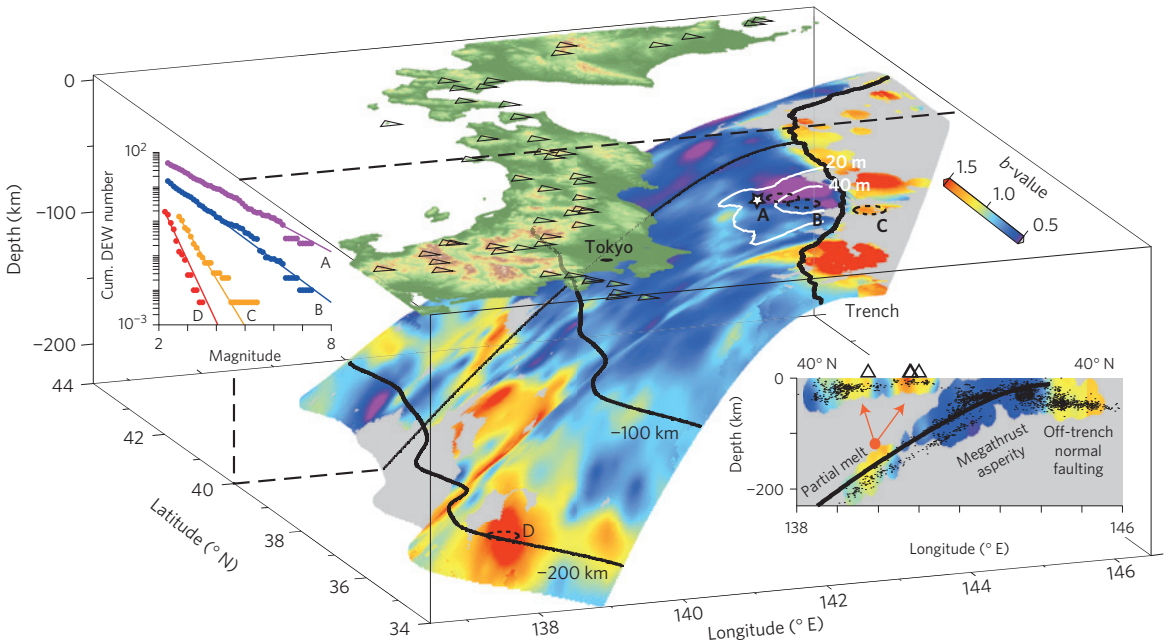

Figure 1 | Three-dimensional study overview. Pre-Tohoku-oki (T2) *b*-values resolved along the subduction interface: high *b*-values in the low-stress normal-faulting off-trench area; low and very low *b*-values along the megathrust. Star: 2011 M9 epicentre. White contours: slip model[22] indicating the M9 highest slip area (previously locked, highly stressed asperity, reflected by very low *b*-values); high *b*-values in the magma source region at depth (dehydration and partial melting). Triangles: volcanoes. Insets: frequency–magnitude distributions (FMDs) for annotated nodes (A, B, C and D) from different tectonic regimes, and cross-sectional view at 40° N, as indicated, showing the relation between *b*-values for subduction and crustal seismicity and surface volcanism. DEW, distance exponential weight.

to ∼100 km, which is consistent with the suggested extent of a further deep coupled zone of high-stress accumulation beneath Japan[16]. Thermal conditions would suggest that stresses here are predominately released aseismically, possibly in decades-spanning slip episodes following shallow megathrust events[16]. However, we have no firm insight from our analysis if this is indeed the case, or if the area can also rupture co-seismically in rare large events.

Third, along the outer rise, the off-trench region that has no continental crust sitting atop exhibits lower differential stresses typical for a shallow normal-faulting regime[17]. This is reflected by comparatively low seismicity rates and high *b*-values ($b > 1.1$). The precise delineation of the steep *b*-value gradient from low to high remarkably follows the trench line.

Temporal variation: asperity loading and unloading

Considering different periods, we find time-dependent signals that are consistent with tectonic stress accumulation and release. We select four periods that separate data before, in between, and after very large events (Fig. 2): T1—before the rupture of the Tokachi-oki M8 event, T2—three months after Tokachi-oki up to the Tohoku-oki M9 event, T3—three months of Tohoku-oki aftershocks, and T4—2013 onwards.

We find that the 2003 M8 Tokachi-oki event did occur within the large and persistent low-*b*-value structure off Hokkaido[18]. (Fig. 2T1 and T2), but not in a distinct region of specifically low *b*-values. The local *b*-values in the high-slip area increased only slightly in the aftermath, and returned to the pre-mainshock level and lower within 1–2 years (Figs 2T2 and 3). This suggests that although an M8 event, the earthquake did not release a significant amount of the overall stress that is continuously accumulating along that part of the Pacific plate on a large enough area to host megathrust earthquakes[19]. Although not an intuitive finding, this is consistent with geodetic observations that reflect only minor fluctuations in the subsidence rate related to M7–8 earthquakes over the past 120 years[20], and independent results from co-seismic stress rotation analysis, which concluded a <1% release of the background stress through the M8 Tokachi-oki event[21]. For the Tohoku-oki event, in contrast, the same study found strong stress rotations between pre- and post-mainshock events and estimated a stress release of >80% (ref. 21), which is equally reflected in the *b*-value results discussed below.

As previously suggested[10], we resolve a distinct low-*b*-value structure in the subsequent high-slip area of the Tohoku-oki mainshock, indicating locally a specifically strong stress accumulation (Figs 1 and 2T2). This asperity on the plate interface extends about 200 km north–south and 100 km east–west, reaching *b*-values of less than 0.5. This pattern was not visible before 2003, and seems to have formed over a number of years[10] (Figs 2T1 and 3). Similarly to laboratory observations of low and decreasing *b*-values that could previously be detected as a fault of a few centimetres length approached failure[4], we find this for natural earthquakes with fault sizes of hundreds of kilometres. However, the timing of this long-term precursory signal remains unexplained, as well as the observation that some low-*b*-value patches emerge and subside without the occurrence of significant ruptures. Because large earthquakes, for example, the 2003 Tokachi-oki event, do not necessarily occur in regions of extremely low *b*-value either, we cannot yet make conclusions about the quantitative predictive power of *b*-value mapping.

In Figs 1 and 2, we show the spatial correlation of low pre-mainshock *b*-values and high subsequent slip with respect to the Yagi and Fukahata slip model[22]. As demonstrated in Fig. 4, this trend of highest slip in the lowest-*b*-value regions is not sensitive to the chosen slip model; we tested four more slip models[23–26], and all confirm the trend. Because largest slip would be expected in volumes of highest previous stress and highest slip deficit, this low-*b*–high-slip correlation provides another strong piece of evidence that low-*b*-value structures can be usefully interpreted as mapping asperities[9]—that is, largely locked, hard-to-break segments that can sustain high levels of stress and tend to release the accumulated slip

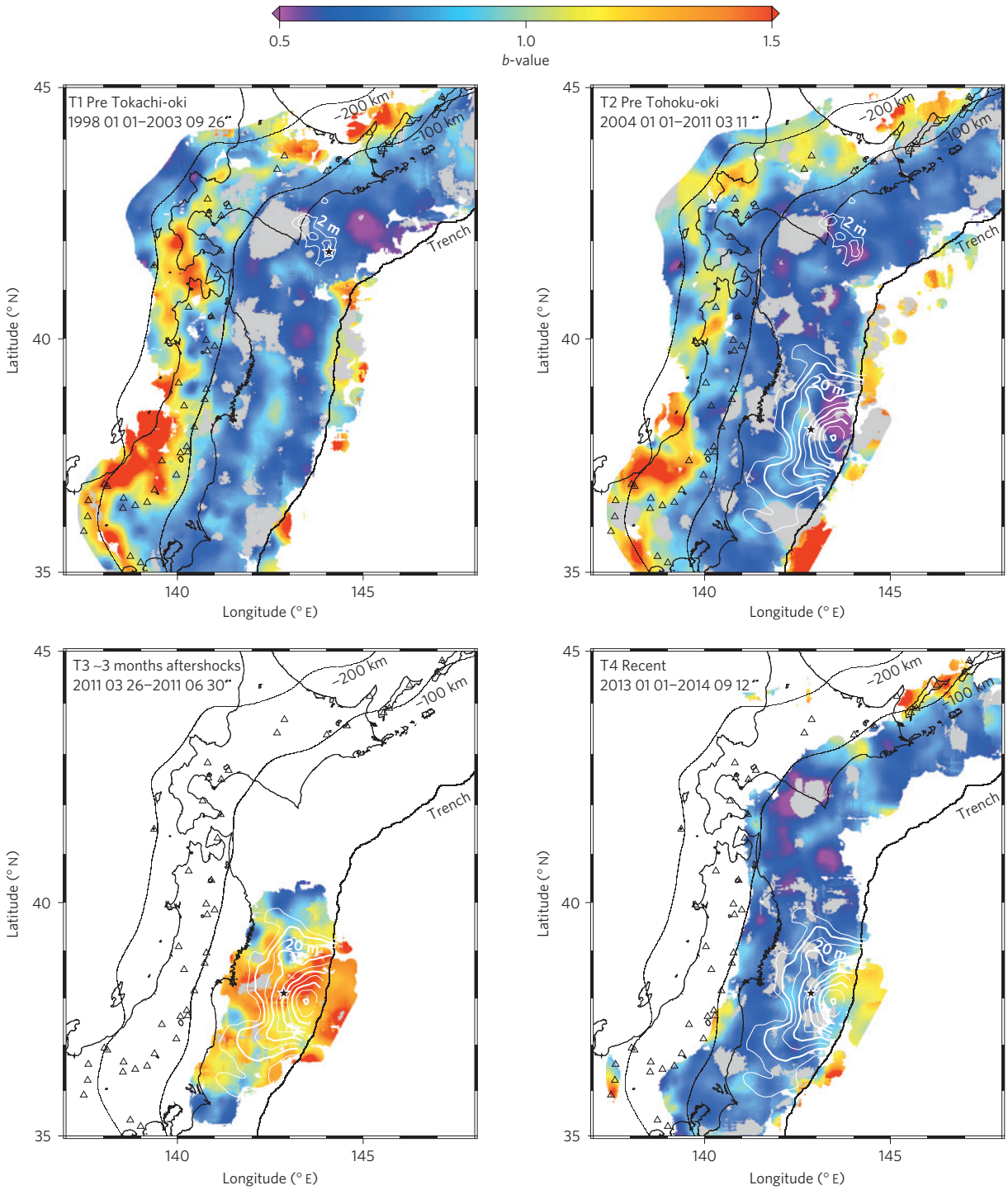

Figure 2 | Temporal evolution of *b*-values along the subducting plate. Mapview along the three-dimensional slab structure for time periods T1–T4. Grey nodes: nonlinear FMDs (ref. 7), stars: 2003 M8 Tokachi-oki and 2011 M9 Tohoku-oki epicentres, white contours: mainshock slip models, 2 m and 4 m for Tokachi-oki[49], 5–50 m for Tohoku-oki[22]. The maps show the first-order, time-independent tectonic imprint on *b*-values and the second-order temporal variation imposed by the M9 mainshock. We note that the apparent shift in the depth of the high-*b*-value band between T1 and T2 might possibly be an artefact caused by network and depth determination changes at that time.

deficit in large ruptures. A different terminology for this observation is that low *b*-values indicate areas of strong coupling—for example, reported along the Cocos Plate subducting beneath Costa Rica[27]. Strongly coupled zones have also been suggested for the Tohoku area pre-2011 (ref. 14), consistent with the observed low *b*-values.

Apart from the low *b*-values before the rupture, we find that areas of large co-seismic slip during the Tohoku-oki event exhibit a significant increase in *b*-values after the mainshock, representing a strong stress release in these areas[21,28] (Figs 2T2 and T3 and 3). Again, the different slip models are consistent with respect to this property (Fig. 4).

We find that *b*-values north and south from the major rupture area are still persistently low after the Tohoku-oki event, and partly even decreased (Figs 2T3 and T4). This is consistent with the stress

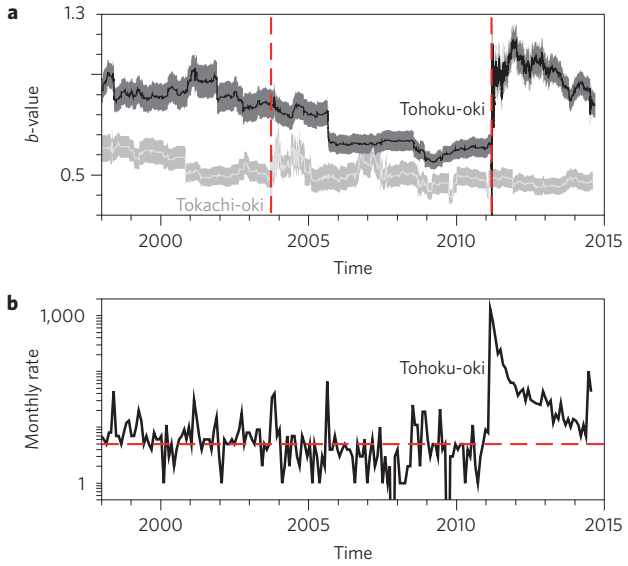

Figure 3 | *b*-value time series and monthly activity rates. a, *b*-value and uncertainty[48] for the Tokachi-oki and Tohoku-oki earthquakes (red dashed vertical lines) (for sampling parameters see Methods). **b**, $M \geq 3$ events per month inside the Tohoku-oki 10-m-slip contour[22], red dashed line indicates the average rate for 1998–2011.

transfer from the major event[29]; in particular, the analysis suggests constant or even increased stress accumulation towards the north, offshore Hokkaido, where the potential for megathrust events has been repeatedly suggested[19]. We also map large areas of persistently low *b*-values further south, offshore and beneath the greater Tokyo area, which has experienced significant seismicity rate increases post-Tohoku[30].

Furthermore, apart from one small region in the northern half of the pre-Tohoku lowest-*b*-value asperity, the high aftershock *b*-values in all of the greater mainshock rupture area and down-slab decrease significantly following the first few months of aftershocks (Figs 2T3 and T4 and Supplementary Fig. 3). Assessed within the 10-m-slip contour, the average *b*-value increase between T1 ($b_{10m\_T1} = 0.81 \pm 0.02$) and T3 ($b_{10m\_T3} = 1.08 \pm 0.04$) has been recovered by ~77% in T4 ($b_{10m\_T4} = 0.87 \pm 0.03$). This might seem surprising on such a short timescale, as it indicates that stress conditions are noticeably rebuilding in the greater asperity area within three years from the M9 earthquake. However, the inference of a rapid stress recovery is consistent with a similarly interpreted observation from post-mainshock stress rotations, which suggest a reloading of the asperity on the order of 6% of the stress drop within the first eight months[21].

To better understand the medium-term impact of the Tohoku-oki event on *b*-values, we assess the observed changes between pre-Tohoku-oki and 2013 onwards (between T1 + T2 and T4), and compare those changes with the *b*-value differences observed between pairs of two-year-long subsets of the catalogue—that is, periods that are not dominated by large earthquake sequences. We add to this comparison the strong changes observed between pre-Tohoku-oki and the first three months of aftershocks (T1 + T2 versus T3), and also the impact of the Tokachi-oki event (Fig. 5).

The range and frequency of observed *b*-value changes between the different periods (Fig. 5) confirm the partly unexpected conclusions: spatio-temporal fluctuations in *b*-values are found to be common in all two-year reference periods, and the impact of the Tokachi-oki event is only of the order of that 'background fluctuation'—that is, it did not alter the stress field significantly; as expected from the above analysis, there is a strong immediate impact of the Tohoku-oki event; and the changes that we document for the 2013-onward period have already significantly subsided towards background levels, with the patch of remaining elevated *b*-values in the northern half of the Tohoku asperity showing up as higher amplitudes for large *b*-value increases compared to the 'background fluctuation' (Fig. 5).

Potentially underlying physical processes

The *b*-values at the end of the study period have returned to values similar to those seen between 1998 and 2003 (Figs 2, 3 and 5). This recovery occurs in the same period of time it takes the aftershock rate to reach the average long-term level (Fig. 3). Together these imply a relatively rapid return over a few years to long-term stationary loading conditions. Even the high tectonic loading rates along this plate boundary alone are probably insufficient to explain such rapid early stress recovery. However, observations of significant coastal uplift[20] post-Tohoku-oki indeed suggest that the proposed deep coupled zone[16] might have started moving aseismically after the megathrust event, possibly contributing to reloading the asperity above[21]. Because the processes at depth are still poorly understood, and post-seismic strength and stress recovery are likely to be locally complex and nonlinear, it would be dangerous to extrapolate the *b*-value trend linearly into the future. It is speculative whether the remaining stress difference will indeed be recovered within a few years, as suggested by the present trend, or will take considerably longer to rebuild.

It remains uncertain if the *b*-value recovery translates linearly into a stress recovery of the same order[3]. Indeed, the correlation between *b*-value and stress as observed in laboratory experiments[3,4], and indicated by this and previous seismicity studies[6–8], is not unique: what drives the increase of the relative frequency of large events in a particular area—that is, the likelihood that small asperities preferably break together, rather than one by one[7,15]? Whereas the stress level is an intuitive key parameter, other different factors have been suggested to play a role, such as the degree of material heterogeneity[31], or the degree of stress concentration (proportional to the product of stress and the square root of the length of the nucleating fracture)[32]. Massive ruptures and subsequent healing and coupling mechanisms might change structural properties locally—that is, close to the main rupture plane. It is difficult, however, to imagine how the structure changes back and forth over larger volumes on the timescales on which *b*-value changes have been documented. Overall, structural and material properties at depth are even more difficult to infer and confirm than stress conditions, and both might to some degree be coupled and depend on each other.

Physical modelling might help to investigate and constrain what components of the stress field imprint on the *b*-values most strongly. The influence of the stress amplitude could be coupled to the degree of homogenization or correlation of the stress field: neighbouring locked patches could possibly move together, producing larger magnitudes, if they are tied by stresses of the same order and direction. Numerical modelling predicts that as a system approaches system-level failure, individual ruptures become progressively more correlated, meaning events occur closer together and grow larger, thus the *b*-value decreases[5]. With the high convergence rate along this plate boundary, such harmonization of the stress field, as part of a fault healing mechanism, might be possible on short timescales, and could be the dominant physical process behind temporal *b*-value variation.

Inference on megathrust recurrence models

Our results indicate that the imprint of the Tohoku-oki event strongly affects the earthquake size distribution, but for a surprisingly limited period. The *b*-value and stress heterogeneity[21] recovery are supplemented by an equally quick decay of seismicity rates, which by mid-2014 have returned to <50% above the

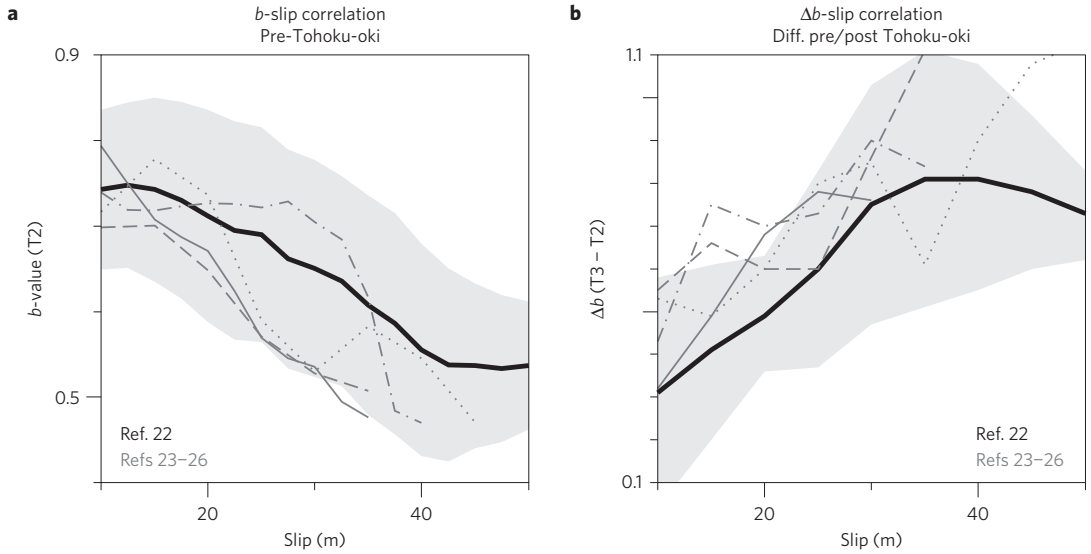

Figure 4 | Correlation between *b*-values and co-seismic slip in Tohoku. *b*-values estimated in 10-m slip bins, overlapping by 5 m, comparing different slip models. Black line and grey shading: mean and standard deviation obtained for the slip model of ref. 22 shown in Figs 1 and 2, dark grey lines: mean for four alternative tested slip models[23–26]. **a**, Pre-Tohoku-oki (T2) *b*-values compared with subsequent slip values, high slip was observed in areas of low *b*-values. **b**, Correlation between slip and changes in *b*-value after the Tohoku-oki event (T3 versus T2), regions of high slip show significant increase in *b*-value.

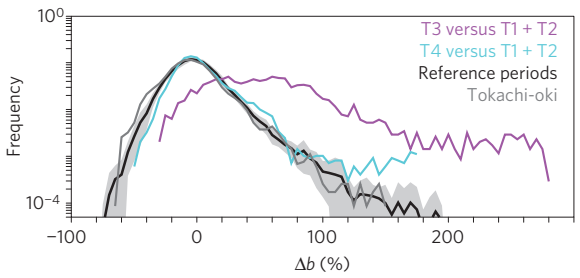

Figure 5 | Significance of temporal *b*-value changes. Histograms of observed *b*-value changes between different time periods. Cyan: T4 versus T1 + T2, magenta: T3 versus T1 + T2, dark grey: two years post- versus pre-Tokachi-oki (without first three months of aftershocks), black line and grey shading: mean and standard deviation of changes observed between six pairs of consecutive two-year periods that are not dominated by large earthquakes (±2 years from 2000, 2001, 2006, 2007, 2008 and 2009).

background rate within the 10-m-slip area (Fig. 3). This is fully consistent with the theoretically expected and observed anti-correlation between aftershock duration and tectonic loading rates: the faster the loading, the shorter the period of aftershock activity[17,33]. Although the stress recovery process is probably heterogeneous in space, and pockets of particularly high or low stress[30] might exist below the resolution of our *b*-value imaging, we see no evidence for a lasting large-scale low-stress regime along the ruptured plate interface, such as would be expected from the seismic gap hypothesis[34]. Specifically, we hypothesize that the Tohoku-oki event might be neither characteristic in location and size, nor in a temporal sense.

Our *b*-value analysis suggests that, although with some degree of local variation and temporal fluctuation, this megathrust zone is more or less constantly and everywhere highly stressed, possibly ready for large earthquakes any time with a low but on average constant probability[35]. We also find no indication for a long-assumed lateral segmentation of the megathrust plate interface into smaller areas that would only rupture in isolation and limit the maximum magnitude[36]. This absence of identified barriers is consistent with the occurrence of the Tohoku-oki event, with its much larger magnitude than anticipated by some[37,38]. The resolved *b*-values thus suggest that future ruptures may involve variable portions of the megathrust, possibly overlapping with the Tohoku-oki rupture plane, and equally likely extend towards the north or south. Consequently, our results suggest that the renewal process along this subduction zone is better described by a stationary Poissonian process rather than a characteristic, partially time-predictable one[39]: a similar size megathrust event is potentially possible in overlapping volumes sooner than expected from estimated mean inter-event times of past events[40], whose variability along the Pacific plate is large[22,40], and possibly supporting a random occurrence hypothesis.

A longer palaeoseismic record along the Cascadia subduction zone showed no evidence for characteristic recurrence either, but suggested a clustered recurrence model[41]. Such behaviour would be equally consistent with the results of our analysis, and could explain how the long-term slip budget is balanced, as the high convergence rate (~8 cm yr^{-1}, >1,100 yr interval) suggests a still significant slip deficit along most of the ruptured plate even post-Tohoku-oki.

A non-characteristic recurrence hypothesis for megathrust events on the Pacific plate is in accordance with an independent laboratory study on the recurrence behaviour of megathrust events in two types of subduction zones[42]: for a model with down dip segmentation, where ruptures cannot reach the trench, characteristic ruptures evolve, whereas on an unsegmented interface the evolving events occur randomly.

In prospect, both the first-order spatial imprint of the large-scale tectonics and the transient changes in *b*-values imposed by the M9 mainshock provide substantial information on the stress field evolution that is at present not considered when evaluating seismic hazard[30]. This could be directly integrated to improve future generations of probabilistic seismic hazard assessment.

Methods

To study the spatial variation of relative stress conditions along the subduction interface, we analyse *b*-values using the Japan Meteorological Agency (JMA) earthquake catalogue along a roughly 1,000 km-long stretch of the Japanese Pacific plate, following the three-dimensional geometry of the subducting slab[43] (Fig. 1).

Completeness magnitude, M_c. *b*-value analysis is critically dependent on a robust estimate of completeness of the processed earthquake data. In particular, underestimates in M_c lead to systematic underestimates in *b*-values[44]. As discussed in other studies[45], M_c of the JMA earthquake catalogue improved

significantly from 1998, when JMA started processing earthquake data recorded by other Japanese institutions. We processed nearly 320,000 earthquakes, starting in 1998, with $M \geq 2.0$, and assessed the temporal and spatial history of $M_c(x,y,t)$ locally at each grid node (Supplementary Fig. 1). M_c varies locally and through time, and very strongly early during aftershock sequences of large earthquakes. We therefore did not consider the first two weeks and three months of Tohoku-oki and Tokachi-oki aftershocks, respectively. For each of the time periods we used a general cutoff (2.0 before Tohoku-oki, 3.7 for the aftershocks, and 2.0 since 2013). We then estimated M_c locally for each node of our 2 km-spaced grid using the maximum curvature criterion[6] and added an extra 0.2 (ref. 44; Supplementary Fig. 1). Sensitivity tests showed that the interpreted structures are stable over a wide range of cutoff magnitudes.

DEW sampling parameters and *b*-value estimation. Because the local stress field primarily influences nearby earthquakes and should have a decaying impact as a function of distance from a considered location, our *b*-value mapping uses distance exponential weight (DEW) sampling[7], which assigns each earthquake an exponentially decaying, distance-dependent weight, w, according to its distance, r, from the considered grid node: $w(r) = 0.7e^{-0.07r}$ (for example, an earthquake at 1 km distance has a weight w of 0.65, the correlation length (that is, where half the maximum weight applies) is ~10 km, and at 75 km $w = 0.003$). In such a way, the events that are closest to a grid node gain the highest weight in mapping the local size distribution, whereas distant events are considered with less importance. This technique focuses the resolution on the plate interface, while sampling both interface and intra-slab seismicity that may influence the local stress field. It furthermore reduces the strong smoothing effect of the commonly applied constant radius sampling and improves the resolution of local structures[46].

We note that, as with any seismicity sampling parameter, the choice of the decay parameter is slightly arbitrary[46]. However, it has been shown to clearly resolve strong *b*-value anomalies for a crustal along-fault setting[7,46], and we verified that the interpreted structures in this study are insensitive with respect to different parameter values. One property of this sampling technique and parameter choice is its robustness to the choice of maximum radius (Supplementary Fig. 2).

We sample earthquakes from a spherical volume of 75 km radius around each grid node and calculate local *b*-values using the maximum likelihood estimate[47] from the weighted frequency–magnitude distribution (FMD; ref. 7). We require 50 or more events above M_c, at least one event located closer than 25 km, and we use a maximum of the 500 closest events per node. The standard deviation[48] of *b*-values decreases with the number of events, ranging from ~15% for 50 events to ~5% for 500 events[46]. We interpret only the *b*-value patterns that are significant well beyond the associated uncertainties, and we exclude from our *b*-value analysis nodes for which the local FMD does not follow a single exponential law[7] (grey areas in Fig. 2).

For time-series analysis for Tokachi-oki and Tohoku-oki, we use events inside 2 m (ref. 49) and 10 m (ref. 22) slip contours, in the depth intervals 20–100 km and 0–30 km, respectively. Values are calculated from a moving window of 100 and 250 events, respectively, going event by event through the catalogue cut at $M \geq 2.0$ and $M \geq 3.0$, respectively, applying maximum curvature[6] and adding 0.2 (ref. 44) to assess M_c in each time bin, always using >50 events. We note that other than the spatial structures, which are robust with respect to the choice of sampling parameters, the time series are rather sensitive and to be interpreted with caution, and only in direct relation to and supplementing the spatial analysis[50]. Choosing one-step sampling has the disadvantage of producing maximum temporal correlations between neighbouring data points, so they cannot be regarded as independent in further quantitative analysis or inference. However, this sampling ensures that the time series exhibits all fluctuation present in the data—that is, trends do not depend on the arbitrary choice of start time of the analysis, as they would for larger step sizes, which randomly omit or accentuate features/peaks.

Received 25 June 2014; accepted 16 December 2014; published online 3 February 2015

References

1. Reid, H. F. *The Mechanics of The Earthquake. The California Earthquake of April 18, 1906* Vol. 2 (Carnegie Institute, 1910).
2. Gutenberg, B. & Richter, C. F. Frequency of earthquakes in California. *Bull. Seismol. Soc. Am.* **34,** 185–188 (1944).
3. Scholz, C. H. The frequency-magnitude relation of microfracturing in rock and its relation to earthquakes. *Bull. Seismol. Soc. Am.* **58,** 399–415 (1968).
4. Goebel, T. H. W., Schorlemmer, D., Becker, T. W., Dresen, G. & Sammis, C. G. Acoustic emissions document stress changes over many seismic cycles in stick-slip experiments. *Geophys. Res. Lett.* **40,** 1–6 (2013).
5. Kun, F., Varga, I., Lennartz-Sassinek, S. & Main, I. G. Approach to failure in porous granular materials under compression. *Phys. Rev. E* **88,** 062207 (2013).
6. Wiemer, S. & Wyss, M. Mapping spatial variability of the frequency–magnitude distribution of earthquakes. *Adv. Geophys.* **45,** 259–302 (2002).
7. Tormann, T., Wiemer, S. & Mignan, A. Systematic survey of high-resolution *b* value imaging along Californian faults: Inference on asperities. *J. Geophys. Res.* **119,** 1–26 (2014).
8. Schorlemmer, D., Wiemer, S. & Wyss, M. Variations in earthquake-size distribution across different stress regimes. *Nature* **437,** 539–542 (2005).
9. Schorlemmer, D. & Wiemer, S. Microseismicity data forecast rupture area. *Nature* **434,** 1086 (2005).
10. Nanjo, K. Z., Hirata, N., Obara, K. & Kasahara, K. Decade-scale decrease in *b* value prior to the M9-class 2011 Tohoku and 2004 Sumatra quakes. *Geophys. Res. Lett.* **39,** L20304 (2012).
11. Bachmann, C. E., Wiemer, S., Goertz-Allmann, B. P. & Woessner, J. Influence of pore-pressure on the event-size distribution of induced earthquakes. *Geophys. Res. Lett.* **39,** L09302 (2012).
12. Wyss, M., Hasegawa, A. & Nakajima, J. Source and path of magma for volcanoes in the subduction zone of northeastern Japan. *Geophys. Res. Lett.* **28,** 1819–1822 (2001).
13. Van Stiphout, T., Kissling, E., Wiemer, S. & Ruppert, N. Magmatic processes in the Alaska subduction zone by combined 3-D *b* value imaging and targeted seismic tomography. *J. Geophys. Res.* **114,** B11302 (2009).
14. Hashimoto, C., Noda, A., Sagiya, T. & Matsu'ura, M. Interplate seismogenic zones along the Kuril–Japan trench inferred from GPS data inversion. *Nature Geosci.* **2,** 141–144 (2009).
15. Uchida, N. & Matsuzawa, T. Coupling coefficient, hierarchical structure, and earthquake cycle for the source area of the 2011 off the Pacific coast of Tohoku earthquake inferred from small repeating earthquake data. *Earth Planets Space* **63,** 675–679 (2011).
16. Ikeda, Y. *Proc. Int. Symp. Eng. Lessons Learn. from 2011 Gt. East Japan Earthquake, March 1–4 2012, Tokyo, Japan* 238–253 (Japan Association for Earthquake Engineering, 2012).
17. Toda, S. & Enescu, B. Rate/state Coulomb stress transfer model for the CSEP Japan seismicity forecast. *Earth Planets Space* **63,** 171–185 (2011).
18. Nakaya, S. Spatiotemporal variation in *b* value within the subducting slab prior to the 2003 Tokachi-oki earthquake (M8.0), Japan. *J. Geophys. Res.* **111,** B03311 (2006).
19. Kanda, R. V. S., Hetland, E. A. & Simons, M. An asperity model for fault creep and interseismic deformation in northeastern Japan. *Geophys. J. Int.* **192,** 38–57 (2013).
20. Nishimura, T. Pre-, co-, and post-seismic deformation of the 2011 Tohoku-oki earthquake and its implication to a paradox in short-term and long-term deformation. *J. Disaster Res.* **9,** 294–302 (2014).
21. Hardebeck, J. L. Coseismic and postseismic stress rotations due to great subduction zone earthquakes. *Geophys. Res. Lett.* **39,** L21313 (2012).
22. Yagi, Y. & Fukahata, Y. Rupture process of the 2011 Tohoku-oki earthquake and absolute elastic strain release. *Geophys. Res. Lett.* **38,** L19307 (2011).
23. Wei, S., Graves, R., Helmberger, D., Avouac, J-P. & Jiang, J. Sources of shaking and flooding during the Tohoku-Oki earthquake: A mixture of rupture styles. *Earth Planet. Sci. Lett.* **333–334,** 91–100 (2012).
24. Pollitz, F. F., Bürgmann, R. & Banerjee, P. Geodetic slip model of the 2011 M9.0 Tohoku earthquake. *Geophys. Res. Lett.* **38,** L00G08 (2011).
25. Suzuki, W., Aoi, S., Sekiguchi, H. & Kunugi, T. Rupture process of the 2011 Tohoku-Oki mega-thrust earthquake (M9.0) inverted from strong-motion data. *Geophys. Res. Lett.* **38,** L00G16 (2011).
26. Hayes, G. P. Rapid source characterization of the 2011 Mw9.0 off the Pacific coast of Tohoku Earthquake. *Earth Planets Space* **63,** 529–534 (2011).
27. Ghosh, A., Newman, A. V., Thomas, A. M. & Farmer, G. T. Interface locking along the subduction megathrust from *b*-value mapping near Nicoya Peninsula, Costa Rica. *Geophys. Res. Lett.* **35,** L01301 (2008).
28. Asano, Y. *et al.* Spatial distribution and focal mechanisms of aftershocks of the 2011 off the Pacific coast of Tohoku Earthquake. *Earth Planets Space* **63,** 669–673 (2011).
29. Toda, S., Lin, J. & Stein, R. S. Using the 2011 Mw 9.0 off the Pacific coast of Tohoku Earthquake to test the Coulomb stress triggering hypothesis and to calculate faults. *Earth Planets Space* **63,** 725–730 (2011).
30. Stein, R. S. & Toda, S. Megacity megaquakes-two near misses. *Science* **341,** 850–852 (2013).
31. Mogi, K. Magnitude-frequency relation for elastic shocks accompanying fractures of various materials and some related problems in earthquakes. *Bull. Earthq. Res. Inst.* **40,** 831–853 (1962).
32. Sammonds, P. R., Meredith, P. G. & Main, I. G. Role of pore fluids in the generation of seismic precursors to shear fracture. *Nature* **359,** 228–230 (1992).
33. Dieterich, J. H. A constitutive law for rate of earthquake its application to earthquake clustering. *J. Geophys. Res.* **99,** 2601–2618 (1994).

34. Kagan, Y. Y. & Jackson, D. D. Seismic gap hypothesis: Ten years after. *J. Geophys. Res.* **96,** 21419–21431 (1991).
35. Bak, P. & Tang, C. Earthquakes as a self-organized critical phenomenon. *J. Geophys. Res.* **94,** 15635–15637 (1989).
36. Stein, S., Geller, R. J. & Liu, M. Why earthquake hazard maps often fail and what to do about it. *Tectonophysics* **562–563,** 1–25 (2012).
37. *National Seismic Hazard Maps for Japan* (Headquarters for Earthquake Research Promotion, 2005); http://www.jishin.go.jp/main/index-e.html
38. Geller, R. J. Shake-up time for Japanese seismology. *Nature* **472,** 407–409 (2011).
39. Kagan, Y. Y., Jackson, D. D. & Geller, R. J. Characteristic earthquake model, 1884–2011, R.I.P. *Seismol. Res. Lett.* **83,** 951–953 (2012).
40. Kagan, Y. Y. & Jackson, D. D. Tohoku earthquake: A surprise? *Bull. Seismol. Soc. Am.* **103,** 1181–1194 (2013).
41. Kulkarni, R., Wong, I., Zachariasen, J., Goldfinger, C. & Lawrence, M. Statistical analyses of great earthquake recurrence along the Cascadia Subduction Zone. *Bull. Seismol. Soc. Am.* **103,** 3205–3221 (2013).
42. Rosenau, M. & Oncken, O. Fore-arc deformation controls frequency-size distribution of megathrust earthquakes in subduction zones. *J. Geophys. Res.* **114,** B10311 (2009).
43. Hayes, G. P., Wald, D. J. & Johnson, R. L. Slab1.0: A three-dimensional model of global subduction zone geometries. *J. Geophys. Res.* **117,** B01302 (2012).
44. Woessner, J. & Wiemer, S. Assessing the quality of earthquake catalogues: Estimating the magnitude of completeness and its uncertainty. *Bull. Seismol. Soc. Am.* **95,** 684–698 (2005).
45. Nanjo, K. Z. *et al.* Analysis of the completeness magnitude and seismic network coverage of Japan. *Bull. Seismol. Soc. Am.* **100,** 3261–3268 (2010).
46. Tormann, T. & Wiemer, S. Reply to "comment on 'changes of reporting rates in the Southern California earthquake catalog, introduced by a new definition of ML' by Thessa Tormann, Stefan Wiemer, and Egill Hauksson" by Duncan Carr Agnew. *Bull. Seismol. Soc. Am.* **100,** 3325–3328 (2010).
47. Aki, K. Maximum likelihood estimate of b in the formula $\log N = a - bM$ and its confidence limits. *Bull. Earthq. Res. Inst.* **43,** 237–239 (1965).
48. Shi, Y. & Bolt, B. A. The standard error of the magnitude-frequency b value. *Bull. Seismol. Soc. Am.* **72,** 1677–1687 (1982).
49. Yagi, Y. Source rupture process of the 2003 Tokachi-oki earthquake determined by joint inversion of teleseismic body wave and strong ground motion data. *Earth Planets Space* **56,** 311–316 (2004).
50. Tormann, T., Wiemer, S., Metzger, S., Michael, A. J. & Hardebeck, J. L. Size distribution of Parkfield's microearthquakes reflects changes in surface creep rate. *Geophys. J. Int.* **193,** 1474–1478 (2013).

Acknowledgements

We thank J. Hardebeck, S. Jónsson and M. Wyss for feedback on the manuscript. We thank JMA for sharing the earthquake catalogue. Figures were produced with The Generic Mapping Tools http://gmt.soest.hawaii.edu. Part of this study was funded through SNF grant PMPDP2 134174. B.E. acknowledges support from the 'Mega-Earthquake Risk Management' project at the University of Tsukuba.

Author contributions

B.E. obtained, selected and pre-processed the earthquake data sets used in this study and provided expert opinion on the Japanese seismotectonics. T.T. led the design of, implemented and conducted the data analysis, and was responsible for result visualization. S.W. and J.W. contributed to the design of the analysis. J.W. contributed to figure generation. All authors participated in the discussion and interpretation of results and the writing of the manuscript.

Additional information

Supplementary information is available in the online version of the paper. Reprints and permissions information is available online at www.nature.com/reprints. Correspondence and requests for materials should be addressed to T.T.

Competing financial interests

The authors declare no competing financial interests.